Nonlinear Analysis of Three-Dimensional Framed Structures Using Smeared Crack Models

Chaisomphob T.
Associate Professor, Department of Civil Engineering
Sirindhorn International Institute of Technology
Thammasat University, 12121 Pathumthani, Thailand

Hansapinyo C.
Master Degree Student, Department of Civil Engineering
Sirindhorn International Institute of Technology
Thammasat University, 12121 Pathumthani, Thailand

Abstract

The nonlinear finite element analysis is used as a tool to obtain the behavior of three-dimensional reinforced concrete frame structures by utilizing constitutive models of reinforced concrete, called smeared crack models. Timoshenko assumption is adopted to permit the beam to experience shear deformation, which is an important feature in deep beam elements. Effect of geometrical nonlinearity which is significant in the beam with high slenderness ratio is also considered in this analysis. The validity of the present nonlinear finite element analysis is confirmed through the comparisons between the analytical results and the available experimental results reported in the literature.

Introduction

In recent years, reinforced concrete frame structures, especially for high-rise reinforced concrete buildings, have been increasingly constructed in which beam elements are used as the practical elements. To predict the real behavior of these reinforced concrete frame structures under general loadings, an accurate nonlinear three-dimensional analysis is indispensable.

This paper aims to model the nonlinear problems as affected by geometric and material nonlinearities. To include geometric nonlinearity, a large displacement is considered. This requires a large displacement stiffness matrix formulation.

A set of constitutive models based on one-dimensional stress field of cracked concrete and reinforcement is used to describe material nonlinearity [1,2].This is known as a smeared crack model of reinforced concrete element. The nonhomogeneous arrangement of material over the cross-section of the element is allowed by discretizing the cross-section into a number of small cells, as shown in Fig.1

This paper presents the nonlinear finite element formulation of the three-node beam element based on updated Lagrangian approach. The numerical analyses are performed and the results are verified by experimental results. The comparisons indicate a reasonably good agreement.

Finite Element Formulation

All numerical procedures for nonlinear analysis have to start from the basic mechanics principles and a step by step approach is suited to nonlinear analysis of solid bodies. The formulation of incremental theories for nonlinear analysis of a solid begins by dividing the loading path of the body into a number of equilibrium configurations, as shown in Fig.2 [3].

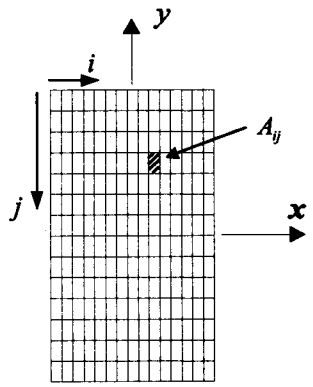

Fig.1 Discretization of the beam cross-section

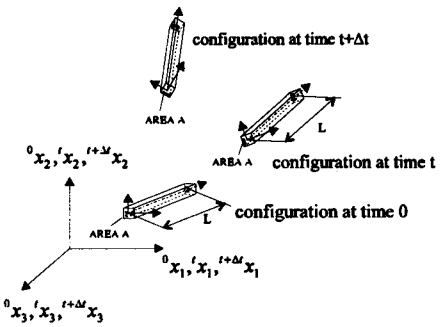

Fig.2: Motion of the three-dimensional beam element and its local co-ordinate axes shown in global co-ordinate system [3]

From [3], it was reported that the updated Lagrangian formulation is efficient in dealing with the beam type structures in terms of the computation efforts required. The principle of virtual displacements based on updated Lagrangian formulation is expressed as

$$\int_{{}^{t}V} {}_{t}^{t+\Delta t}S_{ij}\,\delta\,{}_{t}^{t+\Delta t}\varepsilon_{ij}\,{}^{t}dV = {}^{t+\Delta t}\Re \qquad (1)$$

where ${}^{t+\Delta t}\Re$ is the total external virtual work expression due to the surface tractions and body forces. In Eq.(1), the second Piola-Kirchhoff stress, ${}_{t}^{t+\Delta t}S_{ij}$ is decomposed into the known Cauchy stress, ${}^{t}\tau_{ij}$ and stress increment, ${}_{t}S_{ij}$ Similarly, the Green-Lagrange strain, ${}_{t}^{t+\Delta t}\varepsilon_{ij}$ is decomposed into the known Cauchy's strain, ${}_{t}^{t}\varepsilon_{ij}$ and strain increment, ${}_{t}\varepsilon_{ij}$

Considering ${}_{t}S_{ij}$ and ${}_{t}\varepsilon_{ij}$, which are separated into linear and nonlinear parts, as expressed by

$${}_{t}S_{ij} = {}_{t}S_{ij}^{1} + {}_{t}S_{ij}^{2} \qquad (2)$$

$${}_{t}\varepsilon_{ij} = {}_{t}e_{ij}^{1} + {}_{t}\eta_{ij}^{2} \qquad (3)$$

Using the preceding discussion, Eq(1) can be expressed as

$$\int_{{}^{t}V} ({}^{t}\tau_{ij} + {}_{t}S_{ij}^{1} + {}_{t}S_{ij}^{2})\delta({}_{t}^{t}\varepsilon_{ij} + {}_{t}e_{ij}^{1} + {}_{t}\eta_{ij}^{2})\,d^{t}V = {}^{t+\Delta t}\Re \qquad (4)$$

Due to $\delta\,{}_{t}^{t}\varepsilon_{ij} = 0$ and neglecting higher order terms, Eq.(4) can be expressed as

$$\int_{{}^{t}V} {}_{t}S_{ij}^{1}\delta\,{}_{t}e_{ij}^{1}\,d^{t}V + \int_{{}^{t}V} {}^{t}\tau_{ij}\delta\,{}_{t}\eta_{ij}^{2}d^{t}V = {}^{t+\Delta t}\Re - \int_{{}^{t}V} {}^{t}\tau_{ij}\delta\,{}_{t}e_{ij}^{1}d^{t}V \qquad (5)$$

The constitutive relation between stress and strain increments used now is

$${}_{t}S_{ij}^{1} = {}_{t}C_{ijrs}\,{}_{t}e_{rs}^{1} \qquad (6)$$

Substituting Eq.(6) into Eq.(5) results in

$$\int_{{}^{t}V} ({}_{t}C_{ijrs}\,{}_{t}e_{rs}^{1}\delta\,{}_{t}e_{ij}^{1})\,d^{t}V + \int_{{}^{t}V} ({}^{t}\tau_{ij})(\delta\,{}_{t}\eta_{ij}^{2})\,d^{t}V = {}^{t+\Delta t}\Re - \int_{{}^{t}V} ({}^{t}\tau_{ij})(\delta\,{}_{t}e_{ij}^{1})\,d^{t}V \qquad (7)$$

${}_{t}C_{ijrs}$ in Eq.(7) denotes the incremental constitutive tensor which is the tangent of the curves in the relation between uniaxial tensile stress/uniaxial compressive stress or shear stress with the corresponding strain.

Kinematic Fields of Beam Element

The following assumptions for the beam element are given as follows:

1.After deformation, plane section remains plane, but is no longer perpendicular to the beam axis. This is called Timoshenko beam theory, in which shear strain is constant along the beam section.

2.No deformation in the plane of the cross-section.

3.Warping torsion is negligible.

4.Incremental rotation is small, and can be treated as the vector quantity

By using the above assumptions, the displacements of the generic point A of the beam as shown in Fig.3 can be written as follows:

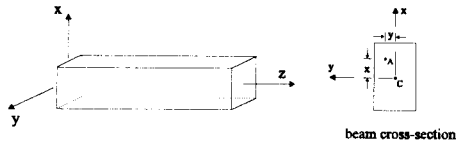

Fig.3 Cross-section of beam

$$u_z = w + y\theta_x - x\theta_y \tag{8}$$

$$u_x = u - y\theta_z \tag{9}$$

$$u_y = v + x\theta_z \tag{10}$$

where u_x, u_y, u_z are the three components of displacement at generic point in x, y and z directions, respectively;

u, v, w are translations at the centroid of beam in x, y and z direction, respectively

$\theta_x, \theta_y, \theta_z$ are rotations about x, y and z axis, respectively

Linear strain increment in Eq.(7) can be written as

$$\begin{Bmatrix} {}_t e^1_{zz} \\ 2\,{}_t e^1_{zx} \\ 2\,{}_t e^1_{zy} \end{Bmatrix} = \begin{Bmatrix} u_{z,z} \\ u_{z,x} + u_{x,z} \\ u_{z,y} + u_{y,z} \end{Bmatrix} \tag{11}$$

Nonlinear strain increment in Eq.(7) can be expressed as

$$\begin{Bmatrix} {}_t \eta^2_{zz} \\ {}_t \eta^2_{zx} \\ {}_t \eta^2_{zy} \end{Bmatrix} = \frac{1}{2} \begin{Bmatrix} (u_{x,z})^2 + (u_{y,z})^2 + (u_{z,z})^2 \\ u_{y,z}u_{y,x} + u_{z,z}u_{z,x} \\ u_{x,z}u_{x,y} + u_{z,z}u_{z,y} \end{Bmatrix} \tag{12}$$

By substituting the preceding expression (Eq.(8)-(10)) for displacements into Eq.(11), (12), the linear and nonlinear strain increments can be written in terms of displacement at the centroid of the beam. Since derivatives of axial displacement and rotations are so small when compared with others, nonlinear strain can be reduced, and finally we obtain

$$\begin{Bmatrix} {}_t e_{zz} \\ 2\,{}_t e_{zx} \\ 2\,{}_t e_{zy} \end{Bmatrix} = \begin{Bmatrix} w' - x\theta_y{}' + y\theta_x{}' \\ u' - y\theta_z{}' - \theta_y \\ v' + x\theta_z{}' + \theta_x \end{Bmatrix} = \begin{bmatrix} 1 & 0 & 0 & 0 & y & -x \\ 0 & 1 & 0 & -y & 0 & 0 \\ 0 & 0 & 1 & x & 0 & 0 \end{bmatrix} \begin{Bmatrix} w' \\ u' - \theta_y \\ v' + \theta_x \\ \theta_z{}' \\ \theta_x{}' \\ \theta_y{}' \end{Bmatrix} \tag{13}$$

$$\begin{Bmatrix} \eta_{zz} \\ \eta_{zx} \\ \eta_{zy} \end{Bmatrix} = \frac{1}{2} \begin{Bmatrix} (u')^2 + (v')^2 \\ 0 \\ 0 \end{Bmatrix} \tag{14}$$

Incremental Stiffness Equation of Beam Element

This study adopts 6-node isoparametric beam element, in which Nodes 1-2-3 represent nodal translation and Nodes 4-5-6 represent nodal rotation, as shown in Fig. 4

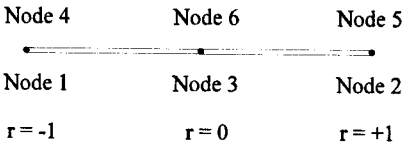

Fig.4 Isoparametric beam element

where

$$N_1 = N_4 = \frac{1}{2}(1-r) - \frac{1}{2}(1-r^2)$$

$$N_2 = N_5 = \frac{1}{2}(1+r) - \frac{1}{2}(1-r^2) \tag{15}$$

$$N_3 = N_6 = (1-r^2)$$

Using the above shape functions torelate displacement function with nodal displacement gives

$$
\begin{aligned}
u&=N_1u_1+N_2u_2+N_3u_3\\
v&=N_1v_1+N_2v_2+N_3v_3\\
w&=N_1w_1+N_2w_2+N_3w_3\\
\theta_x&=N_4\theta_{x4}+N_5\theta_{x5}+N_6\theta_{x6}\\
\theta_y&=N_4\theta_{y4}+N_5\theta_{y5}+N_6\theta_{y6}\\
\theta_z&=N_4\theta_{z4}+N_5\theta_{z5}+N_6\theta_{z6}
\end{aligned}
\qquad (16)
$$

Substituting Eq. (13), (14) and (16) into (7) results in

$$
\left[\int_V [B_i]^T[X]^T[C][X][B_i]d'V+\int_V [B_{ni}]^T[\tau_{zz}][B_{ni}]d'V\right]\{\hat{u}\} \qquad (17)
$$
$$
=\{R\}-\int_V [B_i]^T[X]^T\{\tau\}d'V
$$

Material Models

Uniaxial tensile and compressive stress-strain relationship

For the model of cracked concrete and reinforcing bar subjected to axial force and flexure, the uniaxial model of RC element under tension and compression developed by Okamura and Maekawa[1] is employed as follows

(a) Tensile model

When cracks are generated in the reinforced concrete element under uniaxial stress state, concrete can not support the tensile force at the plane of cracking, and hence bonding between concrete and reinforcing bar becomes significant. Stress distribution of bars and average stress-strain relation in reinforcing bar, and concrete are shown in Fig.4, Fig.5 and Fig.6, respectively

As shown in Fig.6 , The softening curve can be expressed as

$$
\overline{\sigma}_t=f_t\left(\frac{\varepsilon_{tu}}{\varepsilon_t}\right)^c \qquad (18)
$$

where f_t :tensile strength; c = 0.2 for welded mesh and = 0.4 for no welding

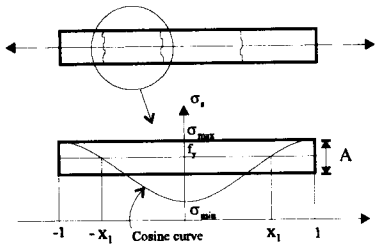

Fig.4 Assumption for stress distribution of bars in concrete [1]

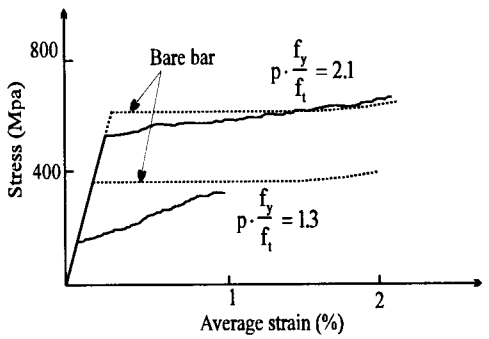

Fig.5 Example of average stress-strain of bars in concrete [1]

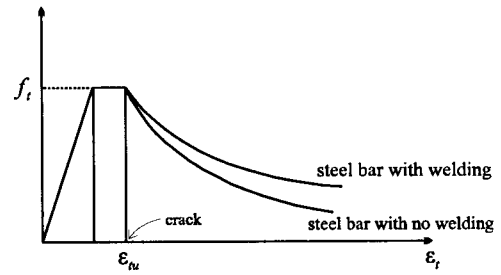

Fig.6 Tension stiffening model of concrete[1]

(b) Compressive model

Based on the concept of the fracture parameter, the relationship between compressive stress and compressive strain in concrete can be obtained, as shown in Fig.7

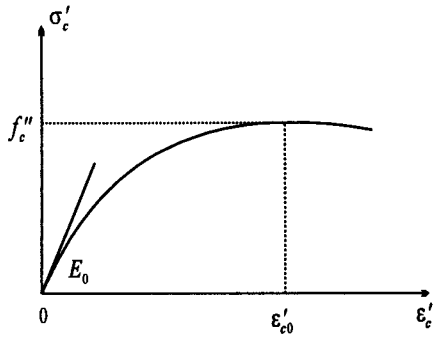

Fig.7 Compressive stress-strain of concrete[1]

For the relationship between compressive stress and compressive strain in reinforcing bar, the stress-strain relationship of bare bar in Fig.5 is used.

Shear stress-strain relations

In this study, the nonlinear relationship of the shear due to flexure will be considered, however the linear relationship due to torsion will be assumed due to large torsional stiffness of reinforced concrete cross-section. At the present state, the shear stress-strain relationship is simply assumed to be similar to tension model shown in Fig.6. It is noted that in the following numerical examples, the failure modes of all cases are flexure one, i.e. shear crack does not occur at failure.

Numerical Precedure

By the iterative Newton-Raphson procedure, the incremental stiffness equation (Eq.(17)) can be solved in order to trace a load-displacement curve of reinforced concrete framed structure. For the sake of simplicity, a load control method is used in this study. In the numerical integration of Eq.(17), the integration along the length of element is performed by a usual Gauss integration technique, and that over the cross-section of element is obtained by taking the sum of the small cells as indicated in Fig.1. It is noted that the accuracy of this integration depends on the size of those cells.

Numerical Examples

Slender hinged beam column

Hinged beam column subjected to eccentric axial loading tested by Abdel-Sayed[4] and Drysdale and Huggins[5] is used to check the validity of the present analysis. The schematic representation of test hinged beam column is shown in Fig.8. These columns were loaded in a short time test up to failure.The comparisons are given in Table 1. The predicted behavior of beam-column number D4 and D7 subjected to eccentric axial loading are shown in Fig.9. From Table 1, the differences of failure load are less than 10%, and as shown in Fig.9, the present analysis can reasonably simulate the load-displacement behavior of the tested beam-column.

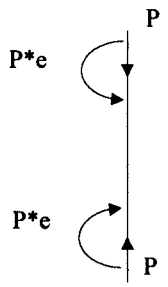

Fig.8 Schematic representation of test hinged Column

Framed structure

Reinforced concrete framed tested by Ferguson [6] is selected in this analysis. The schematic representation of test frame is shown in Fig.10. The principal properties of frame L3 are as follows: compressive strength of concrete is 225 ksc., yield strength of rebar is 4000 ksc. Fig.11 shows the curve of load versus displacement obtained from both experiment and analysis. It can be seen that a good agreement between the experimental and analytical results is also obtained in the framed structure.

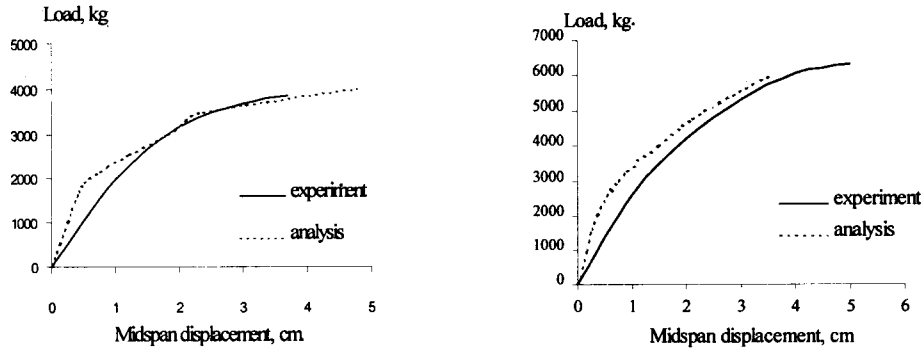

(a) column D4 (b) column D7

Fig.9 Deflection of hinged column

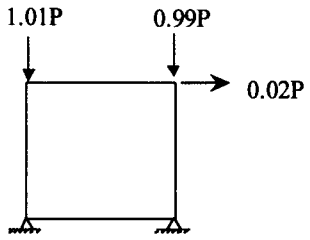

Fig.10 Schematic representation of test frame

Concluding Remarks

The nonlinear finite element analysis of three-dimensional reinforced concrete beam element, considering both geometric and material nonlinearities is presented in this paper.

Slender beam columns under bending combined with axial compression and reinforced concrete framed were chosen to verify the accuracy of the present analysis. The numerical results obtained show a reasonably good agreement with experimental results. The present numerical procedure thus provides a powerful tool for studying the nonlinear behavior of reinforced concrete framed structures. For the next development, an appropriate shear stress/strain relationship will be implemented.

Table 1 Comparison between analytical results and experimental results of hinged column

Column	e_x (mm.)	e_y (mm.)	f_y (ksc.)	f_c' (ksc.)	Failure load (kg.)		Pexp/Pana (%)
					Exp.	Ana.	
D1	63.5	0.0	4,560	314.3	12,946	12,500	103.57
D2	63.5	31.8	4,560	307.2	10,887	10,000	108.87
D3	63.5	63.5	4,560	309.4	8,716	8,000	108.95
D4	127.0	0.0	4,560	317.8	6,327	6,000	105.45
D7	127.0	127.0	4,560	298.8	3,834	4,000	95.85
A-1-C	17.96	17.96	3,940	273.5	17,668	17,000	103.93
D-1-A	25.40	0.0	3,940	309.4	17,577	19,000	92.51

Note : D1-D7 tested by Abdel-Sayed[4], A-1-C and D-1-A tested by Drysdale and Huggins[5

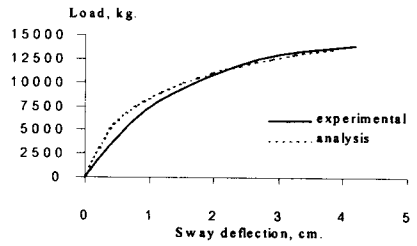

Fig.11 Load versus sway deflection curve

Acknowledgment

The authors would like to express their deepest gratitude and sincerest appreciation to Prof. K. Maekawa, of the University of Tokyo for his advice throughout this study.

References

[1] Okamura, H and Maekawa, K.(1991), Nonlinear Analysis and Constitutive Model of Reinforced Concrete, Giho-do Press, Tokyo, Japan.

[2] Yang, Y. B., and Kuo, S. R.(1994), Theory and Analysis of Nonlinear Framed Structures, Prentice Hall, Singapore.

[3] Bathe, K. J., and Bolourchi, S.(1970), Large Displacement Analysis of Three Dimensional Beam Structures, Int. J. Num. Meth. Engng., Vol.14, pp.961-986.

[4] Abdell-Sayed, S. I. and Gardner, N.J. (1975), Design of Symmetric Square Slender Reinforced Concrete Columns under Biaxially Eccentric Loads, ACI Symposium, Detroit, pp. 149-164.

[5] Drysdele, R. G. and Huggins,M. W. (1971), Sustained Biaxially Load on Slender Concrete Columns, J. Struc. Div., ASCE 97, ST5, pp.1423-1443.

[6] Ferguson, P.M. and Breen (1966), Investigation of the Long Concrete Column in a Frame Subject to Lateral Loads, ACI Special Pub. SP-13, Detroit, MI., pp.75-119.

Appendix

Matrices in incremental stiffness equation(Eq.(17))

$$[X]=\begin{bmatrix} 1 & 0 & 0 & 0 & y & -x \\ 0 & 1 & 0 & -y & 0 & 0 \\ 0 & 0 & 1 & x & 0 & 0 \end{bmatrix}$$

$$[C]=\begin{bmatrix} E_t & 0 & 0 \\ 0 & G_t & 0 \\ 0 & 0 & G_t \end{bmatrix}$$

$$[\tau_{zz}]=\begin{bmatrix} \tau_{zz} & 0 \\ 0 & \tau_{zz} \end{bmatrix}$$

$$\{\tau\}=\begin{Bmatrix} \tau_{zz} \\ \tau_{zx} \\ \tau_{zy} \end{Bmatrix}$$

$$\{\hat{u}\}^T=\begin{bmatrix} u_1 & v_1 & w_1 & u_2 & v_2 & w_2 & u_3 & v_3 & w_3 & \theta_{x4} & \theta_{y4} & \theta_{z4} & \theta_{x5} & \theta_{y5} & \theta_{z5} & \theta_{x6} & \theta_{y6} & \theta_{z6} \end{bmatrix}$$

$$[B_l]=\begin{bmatrix} 0 & 0 & \frac{\partial N_1}{\partial z} & 0 & 0 & \frac{\partial N_2}{\partial z} & 0 & 0 & \frac{\partial N_3}{\partial z} & 0 & 0 & 0 & 0 & 0 & 0 & 0 & 0 & 0 \\ \frac{\partial N_1}{\partial z} & 0 & 0 & \frac{\partial N_2}{\partial z} & 0 & 0 & \frac{\partial N_3}{\partial z} & 0 & 0 & 0 & -N_4 & 0 & 0 & -N_5 & 0 & 0 & -N_6 & 0 \\ 0 & \frac{\partial N_1}{\partial z} & 0 & 0 & \frac{\partial N_2}{\partial z} & 0 & 0 & \frac{\partial N_3}{\partial z} & 0 & N_4 & 0 & 0 & N_5 & 0 & 0 & N_6 & 0 & 0 \\ 0 & 0 & 0 & 0 & 0 & 0 & 0 & 0 & 0 & 0 & 0 & \frac{\partial N_4}{\partial z} & 0 & 0 & \frac{\partial N_5}{\partial z} & 0 & 0 & \frac{\partial N_6}{\partial z} \\ 0 & 0 & 0 & 0 & 0 & 0 & 0 & 0 & 0 & \frac{\partial N_4}{\partial z} & 0 & 0 & \frac{\partial N_5}{\partial z} & 0 & 0 & \frac{\partial N_6}{\partial z} & 0 & 0 \\ 0 & 0 & 0 & 0 & 0 & 0 & 0 & 0 & 0 & 0 & \frac{\partial N_4}{\partial z} & 0 & 0 & \frac{\partial N_5}{\partial z} & 0 & 0 & \frac{\partial N_6}{\partial z} & 0 \end{bmatrix}$$

$$[B_{nl}]_{2*18}=\begin{bmatrix} \frac{\partial N_1}{\partial z} & 0 & 0 & \frac{\partial N_2}{\partial z} & 0 & 0 & \frac{\partial N_3}{\partial z} & 0 & 0 & 0 & ..... & 0 \\ 0 & \frac{\partial N_1}{\partial z} & 0 & 0 & \frac{\partial N_2}{\partial z} & 0 & 0 & \frac{\partial N_3}{\partial z} & 0 & 0 & ..... & 0 \end{bmatrix}$$

$\{R\}$ is the vector of externally applied element nodal loads.